JOURNAL OF CATALYSIS 95, 333–345 (1985)

The Morphology of Rhodium Supported on TiO_2 and Al_2O_3 as Studied by Temperature-Programmed Reduction–Oxidation and Transmission Electron Microscopy

J. C. VIS, H. F. J. VAN 'T BLIK,[1] T. HUIZINGA,[2] J. VAN GRONDELLE, AND R. PRINS[3]

Laboratory for Inorganic Chemistry, Eindhoven University of Technology, P.O. Box 513, Eindhoven, The Netherlands

Received April 10, 1984; revised January 25, 1985

Supported Rh/Al_2O_3 and Rh/TiO_2 catalysts with varying metal loadings were investigated by chemisorption and temperature-programmed reduction and oxidation. Hydrogen chemisorption showed that all the Rh on Al_2O_3 was well dispersed (H/Rh > 1 for loadings below 5 wt% and H/Rh > 0.5 up to 20 wt%), while the dispersion on TiO_2 was much lower. TPR/TPO showed that this was due to the growth of two different kinds of Rh/Rh_2O_3 particles on TiO_2; one kind was easily reduced/oxidized, with a high dispersion, and the other kind was harder to reduce/oxidize, with a lower dispersion. TEM showed that the first kind of Rh_2O_3 consisted of flat, raftlike particles and the second kind of spherical particles.

INTRODUCTION

In the past 10 years or so rhodium has been gaining importance in catalytic chemistry. Not only is rhodium widely recognized as the best catalyst to promote the reduction of NO in "three-way catalysts" (*1–3*), but it also takes a special place in the conversion of synthesis gas, since its product range can include oxygenated products (alcohols, aldehydes, acids) besides hydrocarbons (*4–12*). Various workers have tried to influence the selectivity and activity of supported rhodium catalysts in syngas conversion via a special preparation (*4–6*), via additives (*7–9*), and via control of the oxidation state of the rhodium in the catalysts (*10–12*). In those cases where the influence of additives or mixed oxides worked in the right direction of enhanced oxygenate production, some workers traced this to the presence of rhodium ions on the surface of the catalysts (*12, 13*). The supposed presence of rhodium ions has been a point of discussion for quite some time. Several authors claimed that it was present in monometallic rhodium catalysts. Worley *et al.* investigated among others a 0.5-wt% Rh/Al_2O_3 catalyst via infrared spectroscopy of adsorbed CO (*14–16*), and ascribed several infrared bands to CO molecules bound to isolated Rh(I) sites. This is in contrast with earlier findings by Yates *et al.* (*18*), who investigated some Rh/Al_2O_3 catalysts with electron microscopy and found rhodium to be present as metallic rafts.

In all cases it seems obvious that the support plays an important role in either bringing or keeping the metal in a certain state of (un)reactivity. A special example of such an interaction between metal and support has been described by Tauster *et al.* (*19, 20*) and is now known as strong metal–support interaction (SMSI). Supported noble and transition metals such as Pt, Rh, and Ru are normally capable of chemisorbing among others H_2 and CO. However, if they are supported on oxides such as TiO_2, V_2O_3, and Nb_2O_5, and if they have been reduced at high temperatures (e.g., 773 K), this che-

[1] Present address: Philips Research Laboratories, P.O. Box 80.000, 5600 JA Eindhoven, The Netherlands.

[2] Present address: Koninklijke/Shell Laboratorium, Amsterdam.

[3] To whom correspondence should be addressed.

0021-9517/85 $3.00

misorption capability is greatly diminished. This SMSI phenomenon has been related to the occurrence of lower oxides of the supports (*21*), although these are known to be formed at higher temperatures than necessary to cause SMSI (*22*) and the exact nature of the interaction still remains unclear. The SMSI state can be destroyed according to Tauster *et al.* by oxidation at elevated temperatures, followed by low-temperature reduction (473 K): this procedure restores normal chemisorption behavior (*19*).

All of the above-mentioned phenomena have to do with one common property, namely, the oxidation–reduction behavior of supported rhodium catalysts. We therefore decided to study a number of Rh/Al_2O_3 and Rh/TiO_2 catalysts with varying metal loadings (see Experimental). Al_2O_3 was chosen because it is known as a support giving good dispersions and stable catalysts, and TiO_2 was chosen because it is known to exhibit SMSI. We varied the metal loading to create a variation in particle size, to see whether, and if so how, oxidation–reduction and SMSI behavior are influenced by particle size.

Before we describe the experimental techniques we used, we wish to introduce another topic, namely, passivation. It is obvious that reduced catalyst systems cannot simply be removed from the reduction reactor and then be stored in air for later use; we stabilize (passivate) the metal surface by applying a layer of oxygen upon the metal particles in a controlled way (see Experimental). Although a simple low-temperature reduction is sufficient to remove the passivation oxygen again (as will be shown), some authors have given attention to the state of the catalysts after storage in air. One can see this storage as a prolonged passivation, but without the precautions we take to prevent uncontrollable effects upon the first contact between air and the reduced metal catalyst. Thus Burwell *et al.* used wide-angle X-ray scattering, extended X-ray absorption fine structure (EXAFS), hydrogen chemisorption, and hydrogen–oxygen titration to characterize their supported Pt and Pd catalysts (*23–26*), and they found them to be oxidized to a great extent after prolonged storage in air.

We show that a good insight into all these matters can be gained with the aid of temperature-programmed reduction and of temperature-programmed oxidation (TPR and TPO), supported by chemisorption measurements. TPR as a characterization technique was introduced by Jenkins, Robertson, and McNicol in 1975 (*27, 28*) and has been used extensively in recent years. The development has been reviewed by Hurst *et al.* (*29*). The technique allows one to obtain (semi)quantitative information about the rate and ease of reduction of all kinds of systems, and once the apparatus has been built the analyses are fast and relatively cheap. We used an apparatus as described by Boer *et al.* (*30*), which enabled us to extend the analyses to temperature-programmed oxidation and to gather information about the rate and ease of oxidation as well.

EXPERIMENTAL

TiO_2 (anatase, Tioxide Ltd., CLDD 1367, surface area 20 m^2/g, pore volume 0.5 cm^3/g) and γ-Al_2O_3 (Ketjen, 000-1.5E, surface area 200 m^2/g, pore volume 0.6 cm^3/g) were impregnated with aqueous solutions of $RhCl_3 \cdot xH_2O$ via the incipient wetness technique to prepare the catalysts. Five Rh/Al_2O_3 catalysts were prepared, with Rh contents of 2.3, 4.6, 8.5, 11.6, and 20.0 wt%, respectively. Six Rh/TiO_2 catalysts were prepared, with Rh contents of 0.3, 0.7, 1.0, 2.0, 3.2, and 8.1 wt%, respectively. In the following the catalysts are denoted as RT (Rh/TiO_2) and RA (Rh/Al_2O_3), followed by the metal loading. After impregnation the catalysts were dried in air at 355, 375, and 395 K for 2 h successively, followed by direct prereduction in flowing H_2 at 773 K for 1 h. Prior to removing the catalysts from the reduction reactor they were passivated at room temperature by replacing the H_2 flow by N_2 and subsequently slowly adding

O_2 up to 20%. Then the catalysts were taken out of the reactor and stored for further use.

In our TPR–TPO apparatus a 5% H_2 in air or a 5% O_2 in He flow can be directed through a microreactor, which is connected to a temperature programmer. H_2 or O_2 consumption is monitored continuously by means of a thermal conductivity detector (TCD). A typical sequence of experiments is as follows:

—The passivated or oxidized sample is flushed under Ar at 223 K.

—Ar is replaced by the Ar/H_2 mixture, causing at least an apparent H_2 consumption (first switch peak).

—The sample is heated under Ar/H_2 flow at 5 K/min to 873 K.

—After 15 min at 873 K, the sample is cooled at 10 K/min to 223 K.

—The reduced sample is flushed with Ar.

—Ar flow is replaced by the Ar/H_2 mixture once more, now causing only an apparent H_2 consumption (second switch peak).

An identical sequence is followed during TPO, so the final oxidation temperature in TPO is also 873 K, unless stated otherwise.

The switch-peak procedure deserves some closer attention. The strong signal we call the first switch peak is due mainly to the displacement of Ar by Ar/H_2 in the reactor, but in some cases real hydrogen consumption may take place, even at 223 K. Therefore, we repeat the whole procedure after the TPR has been performed: in that case the catalyst has been reduced and cooled down to 223 K, and as a consequence it is covered by hydrogen. Then we replace the Ar/H_2 by pure Ar. Subsequently we switch back to Ar/H_2. Since we cannot expect any hydrogen consumption from the reduced, hydrogen-covered sample this time, the resulting second switch peak is due solely to the displacement of Ar by Ar/H_2. Thus the difference between the first and second switch peaks reveals the real hydrogen consumption at 223 K, if there is any.

The reactions that might take place during TPO and TPR are

$$4Rh + 3O_2 \rightarrow 2Rh_2O_3 \qquad (O_2/Rh = 0.75)$$

$$Rh_2O_3 + 3H_2 \rightarrow 2Rh + 3H_2O \qquad (H_2/Rh = 1.50).$$

The quantities in parentheses are the hydrogen or oxygen consumptions in TPR or TPO expected for reduction of bulk Rh_2O_3 or formation of Rh_2O_3 (apart from chemisorption of any kind). In a standard experiment a TPR is done on a passivated catalyst, followed by TPO (on the now reduced catalyst), followed by TPR (on the now oxidized catalyst). To differentiate the temperature-programmed data from the chemisorption data, we have used the symbols H_2/Rh and O_2/Rh for the former data and the symbols H/Rh and O/Rh for chemisorption data.

Chemisorption measurements were carried out in a conventional glass apparatus after reduction of the passivated catalysts at 773 K in flowing H_2 for 1 h, followed by evacuation at 473 K for 1 h. After hydrogen admission at 473 K, desorption isotherms were measured at room temperature. For the RT series, 773 K (high-temperature) reduction will induce SMSI, and so the RT catalysts were also reduced at 523 K (low temperature) to study their normal chemisorption behavior. In measuring the desorption isotherms, desorption became noticeable only at pressures below 200 Torr (1 Torr = 133.3 N/m^2), so we believe that the chemisorption value above that pressure is representative of monolayer coverage (cf. Crucq *et al.* (*31*)).

Transmission electron microscopy (TEM) was carried out on a Jeol 200 CX top-entry stage microscope. Photographs were taken at a magnification of 430,000 and then enlarged further photographically to a final magnification of 1,290,000. TEM measurements were made on samples preoxidized at 900 K. This temperature was chosen because, as TPO measurements show, for some samples this temperature is necessary to cause total oxidation. We chose to examine oxidized samples in

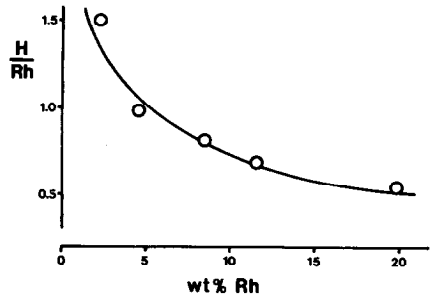

FIG. 1. Hydrogen chemisorption on Rh/Al_2O_3 catalysts as a function of metal loading. T(red) = 773 K.

TEM, since passivated samples may contain rhodium in several oxidation states and this may lead to difficulties (e.g., in electron diffraction). Samples were prepared by applying a slurry of the catalyst in alcohol onto a carbon-coated copper grid and evaporating off the alcohol. Metal loadings were established for the passivated samples spectrophotometrically.

RESULTS

Hydrogen Chemisorption

The hydrogen chemisorption data for the RA series (Rh/Al_2O_3) are represented graphically in Fig. 1, while the data for the RT series (Rh/TiO_2) are presented in Fig. 2. For Rh/Al_2O_3 the H/Rh value drops below 1.0 somewhere around 5 wt% loading, but H/Rh is still above 0.5 at 20 wt% (whose catalyst had to be prepared via two successive impregnation and drying steps). For Rh/TiO_2 reduced at 523 K, H/Rh decreases much faster with increasing metal loading and drops below 1.0 before the metal loading reaches 0.5 wt%. We need to keep in mind the 10 times larger surface area of the alumina, but it is obvious that anatase is less capable of stabilizing small rhodium particles than is alumina. For Rh/TiO_2 reduced at 773 K, some hydrogen chemisorption is still measurable at high metal loadings, but the measured values are of the order of magnitude of the experimental error.

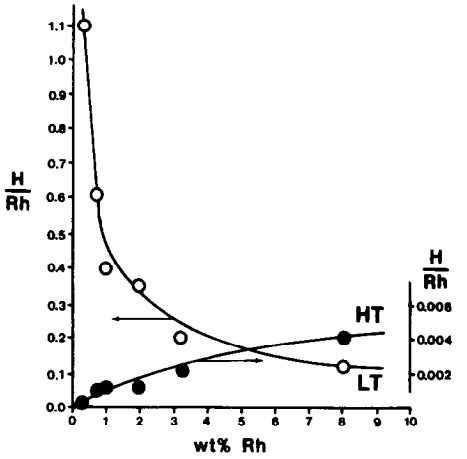

FIG. 2. Hydrogen chemisorption on Rh/TiO_2 catalysts as a function of metal loading. T(red) = 523 K (LT) or 773 K (HT).

The attentive reader will have noticed by now that the catalysts must have already been in the SMSI state after the prereduction at 773 K. The fact that they do show normal chemisorption behavior after 523 K reduction implies that passivation and storage in air have nullified the SMSI.

The reduction–oxidation behaviors of a selected number of these catalysts, RA 2.3, RA 4.6, and RA 20.0, and RT 0.3, RT 1.0, RT 3.2, and RT 8.1, are presented below.

TPR/TPO of the Rh/Al_2O_3 Catalysts

The temperature-programmed reduction profile of a passivated RA catalyst is shown in Fig. 3. The horizontal axis shows the

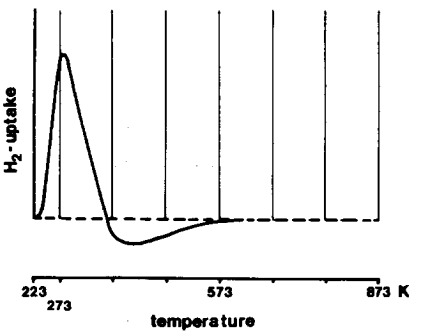

FIG. 3. Temperature-programmed reduction of passivated 2.3 wt% Rh/Al_2O_3.

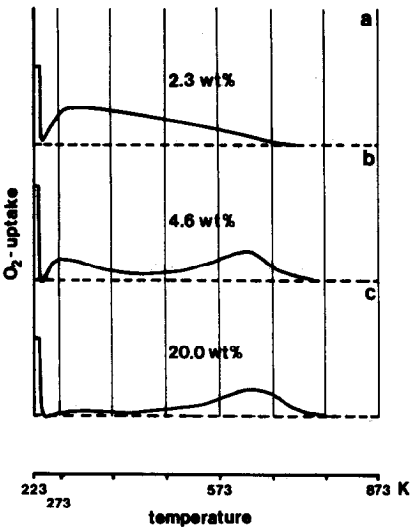

FIG. 4. Temperature-programmed oxidation of reduced Rh/Al_2O_3: (a) 2.3, (b) 4.6, and (c) 20.0 wt%.

temperature, the vertical axis the hydrogen consumption in arbitrary units. All three passivated catalysts show the same profile, with a hydrogen consumption maximum below 300 K, followed by a slight desorption. Hydrogen consumption decreases from 1.33 H_2/Rh for RA 2.3 (which is almost enough to account for the reduction of stoichiometric Rh_2O_3), to 0.49 H_2/Rh for RA 20.0 (average oxidation state of the rhodium in this case was +1).

The subsequent TPO profiles show more difference. For all three catalysts (see Figs. 4a–c), oxygen consumption starts at 223 K, that is, in the switch peak. For RA 2.3 the oxygen consumption rises at the beginning of the temperature ramp, reaches a maximum at 300 K, and falls slowly toward higher temperatures. Total oxygen consumption mounts up to 0.65 O_2/Rh. The behavior of RA 20.0 (Fig. 4c) is quite different. After some oxygen consumption in the switch peak, oxygen consumption keeps a low level for several hundred degrees of temperature rise and reaches a maximum at 628 K. O_2/Rh is 0.70. The behavior of RA 4.6 was intermediate (Fig. 4b). Integration of the oxygen consumption signal proved difficult because of the small thermal conductivity of O_2 and due to the small sample sizes (typically 50–75 μmole of metal).

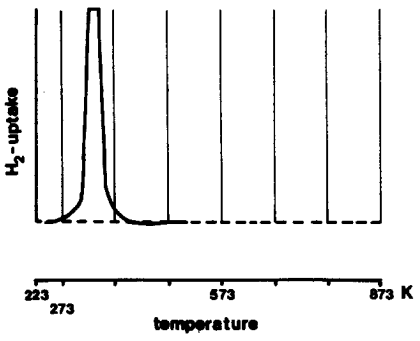

FIG. 5. TPR of oxidized 20.0 wt% Rh/Al_2O_3.

The TPR profiles of all oxidized RA catalysts are similar and the profile of the RA 20.0 catalyst is shown in Fig. 5. The profile consists of one sharp and well-defined peak at about 340 K, with an H_2/Rh value ranging from 1.3 (RA 20.0) to 1.6 (RA 2.3). In all three cases we have the reduction of supported Rh_2O_3. Unsupported Rh_2O_3 in our apparatus showed a reduction peak at 400 K, while bulk rhodium metal only started to become bulk-oxidized above 870 K.

TPR/TPO of the Rh/TiO_2 Catalysts

Figure 6 shows the TPR profiles of the passivated catalysts RT 0.3, RT 1.0, RT 3.2, and RT 8.1. With increasing metal loading, in other words, decreasing H/Rh values, we see how the reduction peak disappears into the switch peak at 223 K. For RT 0.3 the reduction peak is still completely separated from the switch peak, with a maximum at 273 K and an H_2/Rh of 0.56, while for RT 8.1 the reduction peak has merged with the switch peak and the hydrogen consumption has dropped to H_2/Rh = 0.25. We believe that the explanation for this lies in the fact that with decreasing H/Rh (and for RT 1.0 the H/Rh ratio is not more than 0.41, lower than for RA 20.0) the metal particles keep a metallic core upon passivation. Hydrogen molecules can diffuse through the outer passivated layer of the particle, reach the metallic core, and

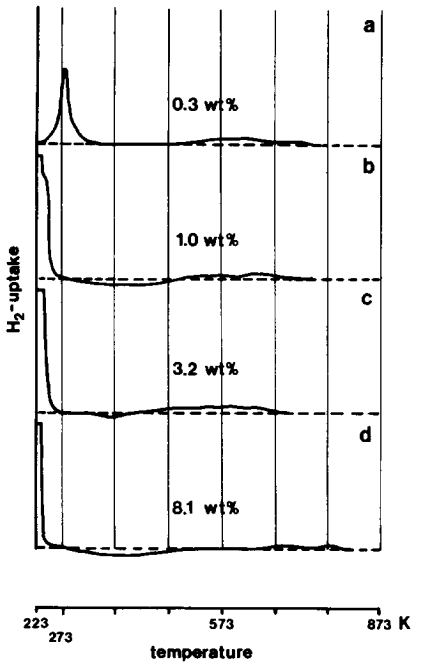

FIG. 6. TPR of passivated Rh/TiO_2: (a) 0.3, (b) 1.0, (c) 3.2, and (d) 8.1 wt%.

dissociate there to provide atomic hydrogen for an easy reduction of the oxide layer at low temperature.

We find support for this idea in Fig. 7, showing the TPO profiles of the respective catalysts. All catalysts show some oxygen consumption as soon as the temperature ramp has been started. The two low-loaded catalysts, RT 0.3 and RT 1.0 (7a and b) have an early consumption maximum around 300 K, like RA 2.3, but also show distinct consumption around 570 K, while RA 20.0 had a maximum around 620 K. In Fig. 7c, RT 3.2, we can distinguish three areas of oxygen consumption apart from the switch peak, namely, around 350, 600, and a new maximum at 770 K. This consumption at 770 K is dominant in Fig. 7d, the TPO of the reduced RT 8.1 catalyst. At first glance we can attribute the low-temperature oxygen consumption to chemisorption and the high-temperature oxygen consumption to thorough oxidation, but we come back to this in the Discussion. In any case, it is this last observation, the high temperature needed for thorough oxidation, that confirms the presence of a metallic core in larger particles after passivation. O_2/Rh is about 0.7 for all RT catalysts.

In Fig. 8, the TPR profiles of the oxidized catalysts are presented, and a very interesting phenomenon shows up here. RT 0.3 and RT 1.0 show only one clear consumption maximum, 330–340 K, H_2/Rh = 1.20, like the RA catalysts (Fig. 5). However, RT 3.2 and RT 8.1 have a second consumption maximum at 385–400 K, about the temperature where unsupported bulk Rh_2O_3 reduces. Taking both peaks together, H_2/Rh is about 1.70 for RT 3.2 and 1.41 for RT 8.1, so without any doubt both peaks can be ascribed to the reduction of Rh_2O_3. To be more specific, the low-temperature TPR peak must belong to well-dispersed, ill-defined Rh_2O_3, which is also easily formed, while the high-temperature TPR peak belongs to the reduction of bulklike, crystalline Rh_2O_3, which can only be formed by the high-temperature oxidation. This was proven earlier (*32*) by halting a TPO experi-

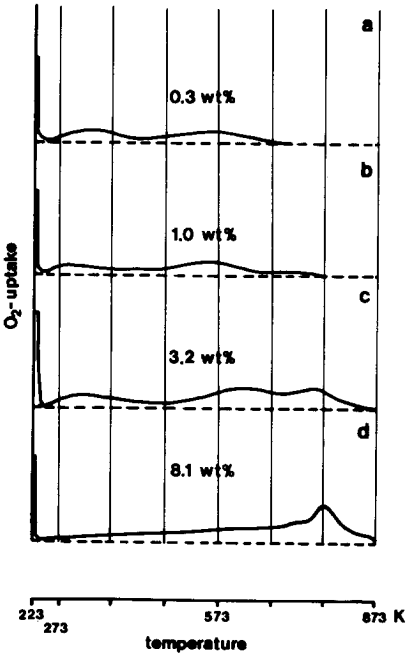

FIG. 7. TPO of reduced Rh/TiO_2: (a) 0.3, (b) 1.0, (c) 3.2, and (d) 8.1 wt%.

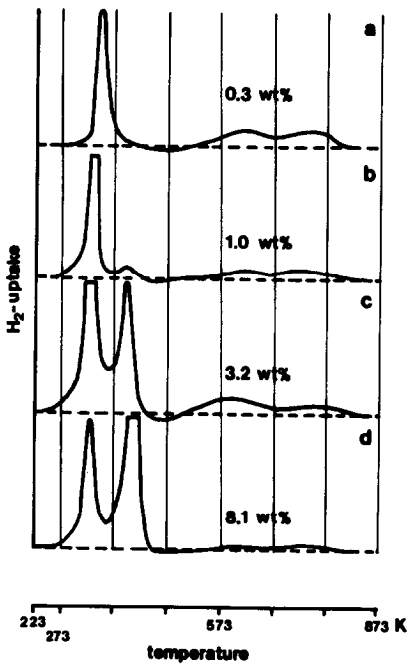

FIG. 8. TPR of oxidized Rh/TiO_2: (a) 0.3, (b) 1.0, (c) 3.2, and (d) 8.1 wt%.

ment at a temperature intermediate between the two maxima at 600 and 770 K. In a subsequent TPR the second reduction peak was missing, so the 770 K TPO peak is connected with the 400 K TPR peak, and the low-temperature TPR and TPO peaks must, as a consequence, be connected too.

In all cases, after a slight desorption of H_2, the H_2 consumption rises again above the baseline, showing two maxima around 600 and 740 K. We attribute this to reduction of the support in the neighborhood of the metal particles; the bare support does not reduce below 800 K.

TEM Measurements

To make the difference between the Rh_2O_3 reducible at 330 K and the Rh_2O_3 reducible at 400 K more clear, we reduced part of the impregnated RT 1.0 batch at 773 K without drying, a method already used by Kobayashi *et al.* (*24*) to prepare catalysts with low dispersions. After oxidation at 900 K for 1 h we performed a TPR, shown in Fig. 9a. A single reduction peak for Rh_2O_3 was observed at 410 K. The subsequent TPO, shown in Fig. 9b, run this time up to 973 K, shows that oxidation proceeds readily only at about 900 K. The H/Rh value of the catalyst, after the 900 K oxidation and a 523 K reduction *in situ*, was 0.20.

We examined this catalyst, RT 1.0 (wet), and the comparable RT 1.0 (Figs. 8b and 7b) catalyst with TEM. Samples were prepared by applying a slurry of the catalysts (oxidized at 900 K) in absolute alcohol on a carbon-coated grid and evaporating the alcohol. TEM micrographs are shown in Figs. 10a–c. Figure 10a shows the bare support, anatase, as received from the manufacturer. It is clearly visible that the TiO_2 particles (with diameters of about 500 Å) are covered with very tiny seed crystals of TiO_2, which apparently, due to the poor sintering capacities of these kinds of oxides, did not have the chance to grow into larger particles. In Fig. 10b (RT 1.0) we find them back as conglomerates (clustered together in the impregnation and drying steps of the preparation) like the one indicated by arrow A. The other particles on the TiO_2 surface show the uniform density and smooth outline characteristic of heavy metal oxide particles, with diameters rang-

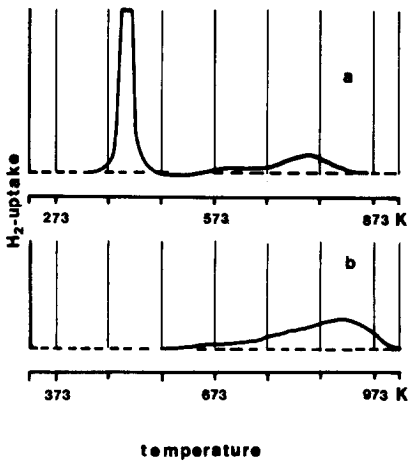

FIG. 9. 1.0 wt% Rh/TiO_2, wet reduced: (a) TPR of an oxidized system and (b) TPO of a reduced system. Note the temperature axis in TPO.

FIG. 10. (a) Transmission electron micrograph of anatase TiO_2; (b) transmission electron micrograph of 1.0 wt% Rh_2O_3/TiO_2 (H/Rh = 0.41); and (c) transmission electron micrograph of 1.0 wt% Rh_2O_3/TiO_2 (H/Rh = 0.2).

ing from 10 to 60 Å. The uniform color of the particles is an indication that these rhodium oxide particles might be flat (raftlike). In Fig. 10c (RT 1.0 (wet)) the TiO_2 conglomerates are no longer visible. Apparently they had the chance during the high-temperature reduction in the presence of water to spread over the surface of the large TiO_2 particles. The particles which we do see are Rh_2O_3 particles. The fact that there is a consecutive light and dark contour around the particles indicates that they are spherical. Their diameter is about 70 Å.

DISCUSSION

Hydrogen chemisorption has been used through the years by many workers to characterize metal surfaces (*6, 11, 13, 17, 19, 23–26, 33, 34*), and when attempts were made to calculate metal surface areas from hydrogen chemisorption data, a hydrogen metal stoichiometry of 1 was always used. On the other hand, if CO was involved, some authors (*35*) chose a stoichiometry of 1, while others (*18*) preferred higher stoichiometries. From Figs. 1 and 2, however,

FIG. 10—*Continued.*

it becomes clear that H/Rh values also can exceed unity. For Rh/TiO_2 this occurs for metal loadings below 0.5%, and for Rh/Al_2O_3 even for metal loadings up to 5%. Although in this study only two catalysts with an H/Rh value above unity were investigated, we have reported about other ultradispersed systems elsewhere (*32, 36*). In our opinion, if one accepts that a metal atom such as rhodium can adsorb two or more CO molecules, one should not reject the idea of that same atom adsorbing more than one hydrogen atom. Thus we also think that in those cases where H/Rh exceeds unity, the hydrogen chemisorbed does not exceed a monolayer (cf. Crucq *et al.* (*31*)) and is all bound to the metal. A consequence of this is the impossibility to calculate a particle size from chemisorption data for highly dispersed systems, since there is no way of calculating the number of rhodium surface atoms. For larger, well-defined particles such as those found in RT 1.0 (wet), with an H/Rh of 0.2, the calculated particle size is 60 Å, which is in good accordance with our TEM measurements (Fig. 10c).

The H/Rh values measured for Rh/TiO_2 after reduction at 773 K (Fig. 2), that is, with rhodium in the SMSI state, seem to

FIG. 10—*Continued.*

show a tendency to increase with metal loading, but the values measured are still sufficiently small that we do not want to draw any conclusions without further study.

From TPR/TPO measurements the following model can be proposed. Rhodium on a support can occur in either a dispersed form or in a bulklike form. The dispersed form is easy to reduce to the metal, giving a reduction peak in TPR around 340 K. It is also easily oxidized, which manifests itself in TPOs such as Figs. 4a and 7a and b, and in the fact that upon passivation the oxidation state of the Rh can almost reach +3 (cf. $H_2/Rh = 1.33$). That reaction with oxygen is vehement, even at room temperature, shows also in the fact that prolonged passivation breaks SMSI (if not, one would not have seen any hydrogen consumption at all after the low-temperature reduction, since the RT catalysts would still be in the SMSI state induced by the 773 K prereduction). The exact assignment of the three TPO peaks is difficult since the literature does not provide much material about the mechanism of oxidation of supported metal catalysts. However, theory, dealing with the oxidation of bulk metals, does envisage three separated phenomena as stages in the oxidation process. Rapid chemisorption is known to occur at clean surfaces (*37*) at low

temperatures. Formation of an oxide film occurs at temperatures typically up to 573–673 K, following logarithmic rate equations, and leading to an oxide film with a thickness from 20 (*38*) to 1000 Å (*39, 40*). Finally, Wagner's oxidation theory (*41*) describes how the oxidation process goes on, rate-controlled by volume diffusion of the reacting ions and/or of electrons through the growing oxide scale, leading to a parabolic rate equation. We can imagine that such models can describe the oxidation processes in supported metal particles as well, dependent on their sizes.

It is observed that the larger supported Rh_2O_3 particles reduce at the same temperature as unsupported Rh_2O_3 (TPR peak at 400 K), while supported Rh metal particles oxidize at a much lower temperature (highest TPO peak at 770 K) than bulk Rh metal (TPO profile just shows beginning of oxidation at 870 K). The reason for this difference in behavior is that during reduction of a metal oxide, diffusion of H_2 is in principle no problem. Diffusion of H_2 through the product metal phase is reasonably fast and the metal phase has a lower specific volume than the reactant metal oxide phase, thus leaving room for H_2 molecules to reach the interface between metal oxide and metal. Therefore in reduction the reduction temperature is determined by the rate of nucleation and thus by the temperature at which a metal oxide can split H_2 at a reasonable rate. On the other hand, in the oxidation of a metal particle the product metal oxide layer is more voluminous than the metal which it replaces, and in many cases a protective product layer will be formed. Oxidation is then fully determined by diffusion and in TPO the peak temperature shifts with particle size. Even for the very highly dispersed catalyst, for which an EXAFS study has shown that on the average each particle only contains 35 atoms (*42*), the TPO profile shows a long high-temperature tail. Apparently also the reconstruction from a chemisorbed state into a pure metal oxide state is an activated process (*43*).

From Figs. 3, 5, 6, and 8 it is clear that no matter how the rhodium is present on the support (dispersed or not, oxidized or passivated) reduction to metallic rhodium is complete at 450 K (Fig. 8) during TPR. With the highest TPR peak maximum in Fig. 8 at about 400 K, it is obvious that Rh on support catalysts will be fully reduced when heated for an hour at 400 K under hydrogen. We cannot conclude from this evidence alone that bimetallic systems such as the Rh/Fe system discussed in the Introduction (*12, 13*) will be metallic at that temperature too. However, in the case of a bimetallic system, reduction tends to take place completely at the temperature where the easier reducible compound would have been reduced in a monometallic system (*44*).

We can conclude from our measurements that the systems which Worley *et al.* have studied (*14–16*) must have been fully reduced prior to admission of carbon monoxide. They found four major infrared absorption peaks: 2100 and 2030 cm^{-1}, called the twin absorption and attributed to a $Rh(I)(CO)_2$ compound; 2050–2080 cm^{-1}, attributed to a Rh(O)CO compound; and 1850–1900 cm^{-1}, attributed to bridged carbonyl species. Also of interest is that the twin absorption peaks are attributed to isolated rhodium sites, since the wavenumbers of these two peaks are independent of CO coverage, unlike the others. For 2.2-wt% rhodium catalysts, they found that Al_2O_3 as a support led to more twin absorption than TiO_2, and $RhCl_3$ as a precursor gave more twin absorption than $Rh(NO_3)_3$. They concluded that $Rh(NO_3)_3$ is more easily reduced than $RhCl_3$, and better still on TiO_2 than on Al_2O_3, thus leaving most unreduced rhodium in the case of $RhCl_3/Al_2O_3$, the catalyst with the most intense twin absorption. We prefer another explanation, since we know that reduction must have been complete in all cases. Rh/Al_2O_3 gives maximum twin absorption because it is the best dispersed system after reduction. Upon CO adsorption the very small rhodium particles

are broken up into $Rh(I)(CO)_2$ species, which give the twin IR absorption. EXAFS proof for this explanation has been published elsewhere (*36*).

Our findings are in good accordance with the results published by Burwell *et al.* for Pd and Pt on SiO_2 and Al_2O_3 (*23–26*). Upon exposure to air larger metal particles form an oxide skin which slows down further oxidation. Logarithmic law-type oxidation is a separate step (Fig. 4c), and thorough (parabolic) oxidation occurs only at 700 K. Apparently diffusion through the oxide layer is strongly hindered.

The finding of two distinguishable phases of rhodium on a support has been reported earlier by Yao and Shelef (*45*), although they used Al_2O_3 as a support. We did not succeed in creating bulklike rhodium on Al_2O_3 by increasing the metal loading in the way that we did in the case of TiO_2, but by wet reduction of the impregnated catalyst it proved possible to make a catalyst which is oxidized above 700 K and reduced at 390 K.

CONCLUSIONS

Hydrogen chemisorption showed very clearly the difference between Al_2O_3 and TiO_2 as supports for rhodium. On Al_2O_3, H/Rh was above 1.0 up to 5 wt% metal loading and was still above 0.5 for 20.0 wt% loading, while in the case of TiO_2, H/Rh dropped below 1.0 before 0.5 wt% loading was reached. The consequences of this difference in dispersion for the behavior of rhodium in oxidation–reduction clearly showed up in TPR/TPO.

On Al_2O_3, Rh_2O_3 is reduced around 340 K, and Rh is oxidized via chemisorption, starting at 223 K, followed by formation of an oxide skin around 630 K. On TiO_2 part of the rhodium behaved in the same way. The other part was harder to reduce (around 390 K) and to oxidize (around 800 K).

With a catalyst prepared by wet reduction (supposed to be sintered), all of the reduction took place at 400 K, and all of the oxidation even above 850 K. TEM showed that the resulting Rh_2O_3 particles were spherical, about 70 Å in diameter, while in an equally loaded, properly reduced catalyst the Rh_2O_3 particles ranged from 10 to 60 Å and showed no sign of a spherical form.

Hydrogen chemisorption did show a tendency at higher metal loadings to survive high-temperature reduction; that is, part of the rhodium seemed to be unaffected by SMSI, but the chemisorption measured was actually too small to draw conclusions from it at present.

The results demonstrate that with a suitable choice of a limited number of techniques one can obtain a very good insight into the state of a catalyst after impregnation and oxidation–reduction.

ACKNOWLEDGMENTS

The authors thank Mrs. A. M. Elemans-Mehring for analyzing the metal content of the catalysts. We are grateful that Mr. D. Schryvers from the RUCA Centre for High Voltage Electron Microscopy in Antwerp was willing to do the TEM measurements for us, and we thank Prof. Ir. J. W. Geus from the University of Utrecht for enlightening discussions on the subject. This research has been supported by the Netherlands Foundation for Chemical Research (SON) with financial aid from the Netherlands Organization for the Advancement of Pure Research (ZWO).

REFERENCES

1. Taylor, K. C., *in* "The Catalytic Chemistry of Nitric Oxides" (R. L. Klinisch and J. G. Larson, Eds.). Plenum, New York, 1975.
2. Kobylinski, T. P., and Taylor, B. W., *J. Catal.* **33,** 376 (1974)
3. Yao, H. C., Yao, Y.-F., and Otto, K., *J. Catal.* **56,** 21 (1979).
4. Ichikawa, M., *Bull. Chem. Soc. Jpn.* **51,** 2268 (1978).
5. Ichikawa, M., *Bull. Chem. Soc. Jpn.* **51,** 2273 (1978).
6. Ichikawa, M., and Shikakura, K., *in* "Proceedings, 7th International Congress on Catalysis, Tokyo, 1980" (T. Seyana and K. Tanabe, Eds.), Part A, p. 925. Elsevier, Amsterdam, 1981.
7. Leupold, E. I., Schmidt, H.-J., Wunder, F., Arpe, H.-J., and Hachenberg, H., *Eur. Pat. Appl.* 0 010 295 A1 (1980).
8. Wunder, F. A., Arpe, H.-J., Leupold, E. I., and Schmidt, H.-J., *Ger. Offen.* 28 14 427 (1979).

9. Bartley, W. J., and Wilson, T. P., *Eur. Pat. Appl.* 0 021 443 (1981).
10. Castner, D. G., Blackadar, R. L., and Somorjai, G. A., *J. Catal.* **66,** 257 (1980).
11. Watson, P. R., and Somorjai, G. A., *J. Catal.* **72,** 347 (1981).
12. Watson, P. R., and Somorjai, G. A., *J. Catal.* **74,** 282 (1982).
13. Wilson, T. P., Kasai, P. H., and Ellgen, P. C., *J. Catal.* **69,** 193 (1981).
14. Rice, C. A., Worley, S. D., Curtis, C. W., Guin, J. A., and Tarrer, A. R., *J. Chem. Phys.* **74,** 6487 (1981).
15. Worley, S. D., Rice, C. A., Mattson, G. A., Curtis, C. W., Guin, J. A., and Tarrer, A. R., *J. Chem. Phys.* **76,** 20 (1982).
16. Worley, S. D., Rice, C. A., Mattson, G. A., Curtis, C. W., Guin, J. A., and Tarrer, A. R., *J. Phys. Chem.* **86,** 2714 (1982).
17. Primet, M., *J. Chem. Soc., Faraday Trans. 2* **74,** 2570 (1978).
18. Yates, D. J. C., Murrell, L. L., and Prestridge, E. B., *J. Catal.* **57,** 42 (1979).
19. Tauster, S. J., Fung, S. C., and Garten, R. L., *J. Amer. Chem. Soc.* **100,** 170 (1978).
20. Tauster, S. J., Fung, S. C., Baker, R. T. K., and Horsley, J. A., *Science (Washington, D.C.)* **211,** 1121 (1981).
21. Baker, R. T. K., Prestridge, E. B., and Garten, R. L., *J. Catal.* **50,** 464 (1979).
22. Huizinga, T., and Prins, R., *J. Phys. Chem.* **85,** 2156 (1981).
23. Uchijima, T., Herrmann, J. M., Inoue, Y., Burwell, R. L., Jr., Butt, J. B., and Cohen, J. B., *J. Catal.* **50,** 464 (1977).
24. Kobayashi, M., Inoue, Y., Takahashi, N., Burwell, R. L., Jr., Butt, J. B., and Cohen, J. B., *J. Catal.* **64,** 74 (1980).
25. Nandi, R. K., Georgopoulos, P., Cohen, J. B., Butt, J. B., and Burwell, R. L., Jr., *J. Catal.* **77,** 421 (1982).
26. Nandi, R. K., Molinaro, F., Tang, C., Cohen, J. B., Butt, J. B., and Burwell, R. L., Jr., *J. Catal.* **78,** 289 (1983).
27. Robertson, S. D., McNicol, B. D., de Baas, J. H., Kloet, S. C., and Jenkins, J. W., *J. Catal.* **37,** 424 (1975).
28. Jenkins, J. W., McNicol, B. D., and Robertson, S. D., *Chem. Tech.* **7,** 316 (1977).
29. Hurst, N. W., Gentry, S. J., Jones, A., and McNicol, B. D., *Catal. Rev.-Sci. Eng.* **24,** 233 (1982).
30. Boer, H., Boersma, N. F., and Wagstaff, N., *Rev. Sci. Instrum.* **53,** 349 (1982).
31. Crucq, A., Degols, L., Lienard G., and Frennet, A., *Acta Chim. Acad. Sci. Hung.* p. 111 (1982).
32. Vis, J. C., van 't Blik, H. F. J., Huizinga, T., van Grondelle J., and Prins, R., *J. Mol. Catal.* **25,** 367 (1984).
33. Sinfelt, J. H., and Yates, D. J. C., *J. Catal.* **10,** 362 (1968).
34. Wanke, S. E., and Dougharty, N. A., *J. Catal.* **24,** 367 (1972).
35. Bhasin, M. M., Bartley, W. J., Ellgen, P. C., and Wilson, T. P., *J. Catal.* **54,** 120 (1978).
36. van 't Blik, H. F. J., van Zon, J. B. A. D., Huizinga, T., Vis, J. C., Koningsberger, D. C., and Prins, R., *J. Amer. Chem. Soc.* **107,** 3139 (1985).
37. Ehrlich, G., *in* "Conference on Clean Surfaces," *Annals. N.Y. Acad. Sci.* **101,** (1963), Art. 3.
38. Cabrera N., *in* "Semiconductor Surface Physics" (R. H. Kingston, Ed.), p. 327. Univ. of Pennsylvania Press, Philadelphia, 1957.
39. Birks, N., and Meier, H. G., *in* "Introduction to High Temperature Oxidation of Metals." Arnold, London, 1983.
40. Kofstad, P., *in* "High-Temperature Oxidation of Metals," p. 41. Wiley, New York, 1966.
41. Wagner, C., *in* "Atom Movements," p. 153. *Amer. Soc. Met.,* Cleveland, 1951.
42. van Zon, J. B. A. D., Koningsberger, D. C., van 't Blik, H. F. J., and Sayers, D. E., *J. Chem. Phys.* **82,** 5742 (1985).
43. Savchenko, V. I., Boreskov, G. K., Kalinkin, A. V., and Salanov, A. N., *Kinet. Katal.* **24,** 983 (1984).
44. Wagstaff, N., and Prins, R., *J. Catal.* **59,** 434 (1979).
45. Yao, H. C., Japar, S., and Shelef, M., *J. Catal.* **50,** 407 (1977).